



Experimental evaluation of RC frames retrofitted by steel jacket, X-brace and X-brace having ductile ring as a structural fuse

Ali Kheyroddin^{1,2} · Reza Sepahrad¹ · Mohammad Saljoughian¹ · Mohammad Ali Kafi¹

Received: 28 September 2018 / Accepted: 5 April 2019 / Published online: 22 April 2019
© Springer Nature Switzerland AG 2019

Abstract

Due to several reasons as the low resistance of constructed concrete and also change in codes or application of structures, some concrete frames need to be retrofitted. By adding the steel brace to the reinforced concrete, many seismic parameters such as resistance, ductility, stiffness and the resistance reduction coefficient change. This study experimentally investigates the impact of adding the prop, the convergent steel brace and also the convergent steel brace with a ductile ring on resistance, stiffness, ductility and energy dissipation of RC frames. Four samples of RC frames with one span and one story with the same characteristics were constructed and retrofitted by different methods. All frames were subjected to the cyclic loading, and the hysteresis and pushover-displacement graphs of them were plotted. The novelty of the work was using such braces in RC frames. The results obtained from the tests showed that although the frame retrofitted by the X-brace showed a better performance in terms of resistance and stiffness, but the retrofitted frame with a ring also showed a better behavior in terms of resistance and stiffness compared to the RC frame and the sample with the jacket as well as compared to the sample with the X-brace showed more ductility and energy dissipation (with a slight reduction in resistance).

Keywords RC moment resisting frame · Retrofitting · X steel brace · Ductile ring · Steel jacket · Hysteresis

1 Introduction

There are several reasons for retrofitting the RC buildings such as a change in guidelines, change in the use of buildings, the addition of floors to buildings or the low strength of concrete which can be motivated by guidelines evolution or revision. These structures need to adapt themselves to new demands or guidelines. Different parameters should be evaluated for retrofitting these structures. So far, many methods have been investigated for the strengthening of structural members [8, 19] and many models were presented by researchers for predicting the behavior of strengthened members [17, 21, 12]. Different guidelines like ASCE 7-05 are available for this purpose [2]. The design guidelines address some specifications and parameters of steel frames by the

engineering judgment and non-linear analyzes. However, these analyzes are very difficult, especially at the contact part of elements between concrete and steel. Advantages such as very high energy dissipation capability and lateral elastic stiffness, as well as appropriate ductility have made the steel shear wall a suitable lateral load bearing system. Compared to the reinforced concrete shear wall, the steel shear wall is substantially lighter and provides the user with more space due to its very small thickness. The steel shear wall functions similarly to a vertically placed plate girder. Videlicet, the beams act as stiffeners, the columns as the flanges, and the steel plate as the web of the plate girder. The basis for the usage of steel shear walls without stiffeners is to utilize the diagonal tensile field, which is created after the steel plate buckles. The phenomenon of diagonal buckling and its employment in the steel shear wall was first proposed in the 80's.

In recent years, many studies have been conducted on retrofitting RC buildings with steel elements. In 1980, Sugana and Fujimara experimentally conducted some studies in the field of using the external brace on a few samples and compared them with masonry and concrete frames and obtained satisfactory results on stiffness and energy dissipation. They

✉ Reza Sepahrad
rezasepahrad@yahoo.com

¹ Department of Civil Engineering, Semnan University, Semnan, Iran

² Member of Center of Excellence for Engineering and Management of Civil Infrastructures, University of Tehran, Tehran, Iran

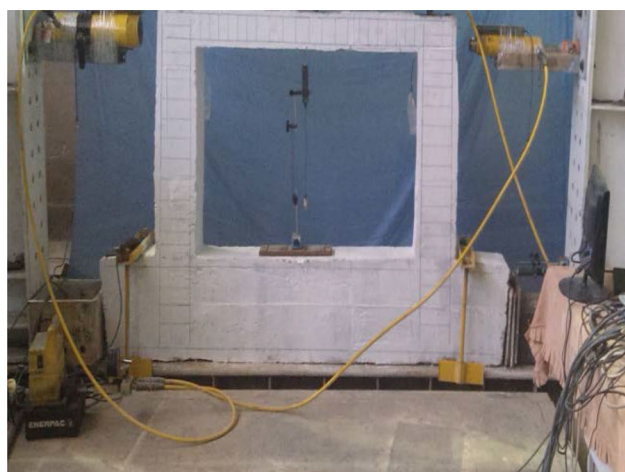
also used this method to retrofit a school in Japan [15]. In 1981, Higasho et al. conducted a study on the application of convergent and out-of-center frames. The results indicated the possibility of the effective use of this retrofitting method [9]. In 1990, Gul and Lee experimentally studied the seismic retrofitting of RC structures using the ductile steel bracing system. The results showed that the retrofitted frame under the cyclic displacements has a good ductility and energy dissipation [7]. In 1991, Weilly et al. presented a report on retrofitting the RC building of the Berkeley University Hall in California with steel bracing. The method used in this project is using the steel frame braced in RC frames. In this report, it is clarified that the used steel bracing system is the most cost-effective method for retrofitting [18]. In 2007, Youssef et al. by conducting two cyclic loading tests evaluated the impact of using the steel brace on a moment frame and a frame with an X-brace. The results showed that compared to the moment frame, the braced frame has a more resistance, adequate ductility and an acceptable seismic performance in general [22]. Saeid and Nahdi provided a method entitled “local bracing system” for retrofitting RC connections. They prepared two samples of RC, which one of them as the reference sample and the other one as the retrofitted sample were subjected under the quasi-static cyclic loading. They studied and compared their behaviors. Their study showed the improvement of the general performance of the retrofitted connection compared to the reference connection [13]. Sharbatdar, Kheyredin, Emami, by providing a modern method using the steel jacket and the steel bracket tried to retrofit some connections which had been defected in terms of resistance due to the elimination a part of the beam height. In their study, first by preparing two connection samples with the scale of 1/2 with different beam heights (15 cm and 20 cm) investigated the impact of the reduction of the beam height on stiffness and energy absorption. Then, by applying the introduced method they retrofitted the mentioned connections after the test and the initial loading. The results of this retrofitting indicated increasing of resistance, local ductility, energy absorption and decreasing of stiffness drop and narrowing the hysteresis loops. Another result of this study is the shift of the plastic hinge in the RC beam from the edge of the beam-column connection to the top edge of the beam drop box. Furthermore, in this method the vertical displacement of the beam is also controlled using the bracket in the service state, however during the cyclic loading of the earthquake causes to improve the seismic factors and consequently the better performance of the RC frame against the loads caused by the impact of earthquake [14]. In the form of a paper, Kheyroddin investigated the hybrid behavior of the shear wall and the steel frame and the braces areas effects on the RC structure behavior and the percent of absorbed shear and the lateral displacement of the structure. For this purpose, a ten-storey RC structure

subjected to vertical and earthquake forces was designed and analyzed. In the first stage, a single moment frame, in the second stage the frame and the shear wall, in the third stage the frame with the shear wall and the steel brace and in the fourth stage the RC frame with the steel brace were studied. The results show that if in a RC structure which has a moment frame and a shear wall and also retrofitted by the steel brace, the lateral displacement exceeds from the allowable limit the braces area can be somehow effective and after that, it does not have a significant impact of the structure behavior. By increasing the braces area, the shear absorption by the frame decreases and after a specified limit the braces do not have any contribution in the shear absorption of earthquake. The behavior of the brace and the frame in the lower and middle floors are almost the same. The comparison of two moment frame systems with and without braces shows that using the steel brace decreases the lateral displacement of the structure down to 50 percent [10]. There were other studies using steel bracing as a technique for retrofitting RC frames in recent years [5, 16, 20].

As discussed, many studies have been conducted on retrofitting RC frames with steel elements to enhance the performance of these braces such as resistance increasing, ductility and energy absorption. However, nothing has been done in applying the ductile ring at the corner of the brace connection to the RC frame and compare this sample with various states, so far. In this regard, four experimental samples including the RC frame, the RC frame with jackets, the RC frame braced with the convergent X-brace, and the RC frame with the convergent X-brace with ductile rings at the bottom corner were constructed. These samples were subjected to the static cyclic loading up to collapse. Based on the hysteresis diagrams of force–displacement of the frames, different parameters including resistance, stiffness, energy dissipation and ductility were evaluated and compared.

2 Test samples and setup

The reference sample is the RC frame shown in Fig. 1. The distance between the columns of the experimental rigid frame is 300 cm from each other, and the height of the rigid frame is about 210 cm. Thus, by considering the length required for applying the load by the jack on both sides and also the suitable distance for the cyclic displacement of frames, the length span of the frame was considered 160 cm. Also, the frame height plus the foundations was considered equal to 140 cm. The foundations of all frames were constructed in the form of a strip, and the space between the foundations and the experimental rigid frames were filled by steel plates to avoid from any movement, displacement, and uplift of the foundation during the test. Also, to make the test frame close to the actual



(a)



(b)

Fig. 1 **a** The reference moment resisting frame and **b** frame reinforcement

structure and create the fixed condition for the support, the foundation was attached to the rigid floor of the laboratory through some rods. The beams with the height of 15 cm and the width of 20 cm and the columns with a square cross-section with a width of 20 cm were selected. The concrete cover was considered equal to 2.5 cm. For the column reinforcing bars, the minimum value of the code equal to 1 percent is used, and four reinforcing bars with a diameter of 12 mm were considered for the columns. For the beam reinforcing bars, two bars with a diameter of 8 mm at the top and two bars with a diameter of 10 mm at the bottom were used, so that the ratio of the beam bars are equal to 0.0085 which met the minimum (0.0035)



(a) MRF-J



(b) MRF-X



(c) MRF-X-R

Fig. 2 Specimens 2, 3 and 4

and maximum (0.025) values of the guidelines (National Building Regulation of Iran [4]). The stirrup placement in the beam and the column was performed compressively to avoid from shear damages in the samples. For stirrups, bars with a diameter of 6 mm were used.

Four samples similar to Fig. 1 were constructed. The concrete specifications and the bar mesh for these samples are similar. There of these frames were retrofitted with different methods shown in the Fig. 2. The naming of the samples is as follows:

Specimen 1 Un-retrofitted RC moment resisting frame (MRF)

- Specimen 2 RC moment resisting frame retrofitted with steel jacket (MRF-J)
- Specimen 3 RC moment resisting frame retrofitted with concentric X brace (MRF-X)
- Specimen 4 RC moment resisting frame retrofitted with concentric X brace along with steel ductile ring (MRF-X-R)

For connection, the steel brace to the RC frame, two methods including direct and indirect can be used. The direct method is used in this test. For welding, the steel brace to the corner connection plate, the steel jackets around the beam and the column are used. Also, for further investigation of the impact of steel jackets, only one frame is equipped with the steel jacket to see its impact on the frame behavior.

Also, for the sample MRF-X-R in which the steel ductile ring has been used, two rings without a gap with a length of 8 cm and a thickness of 8 mm (outer diameter = 114 mm, inner diameter = 98 mm) were welded at the bottom of the brace at the connection point to the corner plate. The first note that should be mentioned is the diameter and the thickness of the ring. Based on this fact that using this ring in the sample is for increasing ductility and avoiding from the brace buckling, the ring should be ruptured along the weld line and not along its line or another line [according to the previous studies noted in the followings (Fig. 3 and Eq. 1)] before the brace is buckled.

$$2M_p = \frac{P \cdot R}{2} \rightarrow P = \frac{4M_p}{R}$$

$$M_p = \frac{I^2 \sigma_y}{4} \tag{1}$$

$$P = \frac{I^2 \sigma_y}{R}$$

M_p : plastic moment of ring, L : length of ring, R : ring radius, σ_y : yield stress.

Also a LVDT was used on the rings that is shown in Fig. 4.

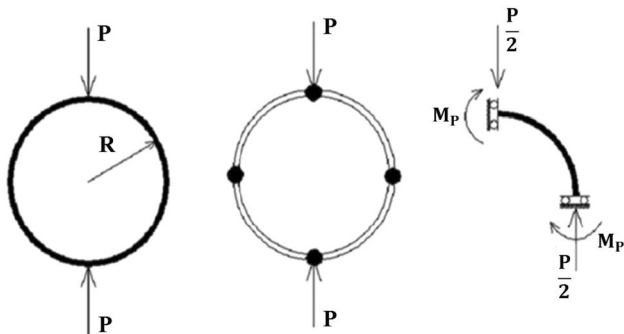


Fig. 3 Steel ring loading and place of plastic hinge formation [1]

A 3*3*0.3 cm double angle with a 3.48 cm² was used for X brace. For the corner connection plate, the middle plate, the brace belts and steel jacket plates around the column and the beam, plates a thickness of 1 cm were used (shown in Fig. 5). All plates were made of ST37 steel. The thickness and the dimension of the plates were calculated by manual and software analyzes.

The steels used in this study are categorized into three groups:

1. The bars used in the RC frame,
2. The angles used for X-brace,
3. Steel plates used for the column and beam steel jackets and the brace corner connections.

In order to determine the bars specifications, one sample from bars 8 and 10 and two samples from bar 12 with suitable length were taken and using the SANTAM STM-400 device with the capacity of 400 kN were subjected to the tensile test in the material laboratory of Semnan University. The results are listed in the Table 1.

In order to determine the angle specifications, due to the inappropriate section of the angle for the test device, first apart from one side of the angle was cut to create a belt, then using a pattern available for testing the steel belt it should be turned. The steel belt prepared for the tensile test is shown in Fig. 6 and the results are shown in Table 2.

In order to determine the specifications of the concrete used in the experimental samples, four concrete samples were taken from each concreting and were tested before the frame test. To this end, the standard cylindrical samples of section 9 of the National Building Regulations [4] with a diameter of 15 cm and a height of 30 cm and also 10*10*10 cubic samples were used (that is shown in Fig. 7). After 28 days, the compressive strength test was conducted on the cylindrical and cubic samples, and the mean strength of 24.8 MPa was obtained.

Two compressive hydraulic jacks were used in both sides and at the top of the frames so that when one jack in one side is pushing, the other jack is in the discharge mode and vice versa. Also, ATC-24 [3] is used for the applied displacements in these tests.

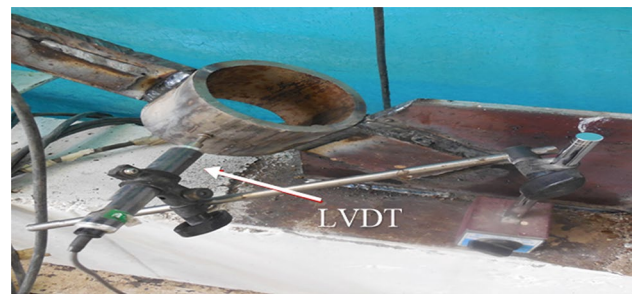


Fig. 4 LVDT on the ring

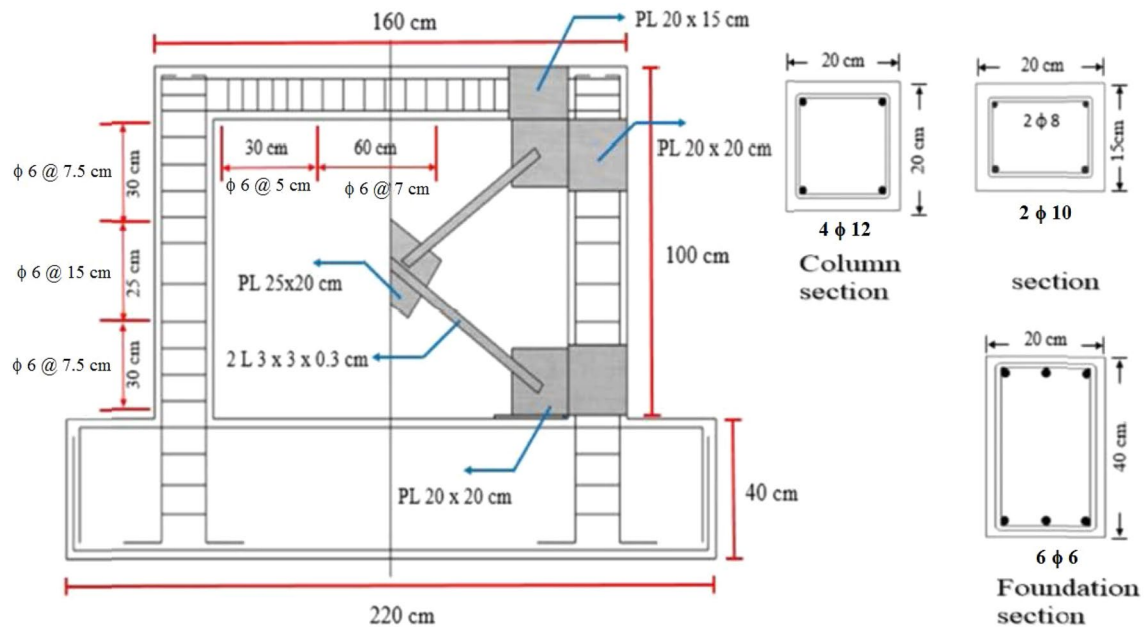


Fig. 5 Details of RC frame, brace and curb

Table 1 The results of the tensile test for bars in specimens 1–4

Specifications				
	Test name	Test mode	Sec. area (mm ²)	Gauge Len (mm)
1	r12.ttd	Tensile	113	120
2	r12-f.ttd	Tensile	113	240
3	R8.ttd	Tensile	50.3	160
4	r10.ttd	Tensile	78.5	200
Results				
	Peak stress (kg/mm ²)	Break strain (%)	Yeild stress (kg/mm ²)	
r12: 1	73.46034	36.6561	55.77838	
r12-f: 2	73.53071	20.2809	56.29108	
R8: 3	54.31428	38.6303	36.97167	
r10: 4	69.17158	22.6947	42.49289	
Delta	19.21643	18.3494	19.31941	
SD	7.881872	8.15259	8.383664	
Mean	67.61923	29.5655	47.8835	

3 Load apply, increasing the number and width of cracks and test results

The hysteresis diagram of force–displacement and the progression of the MRF sample crack in different cycles are shown in Fig. 8. The first crack occurred in the 2.4 mm displacement in the 0.24% drift (the distance of the load

applied to the column base was 1000 mm) at the location of the beam–column connection, and in the 0.5% drift, some cracks were appeared at the column base. Also, in the 1% drift, the first plastic hinge occurred in the bars of the right side column. By increasing the loading, new cracks were appeared and the depth of the previous cracks increased. Then, in the right side loading and the 4% drift,

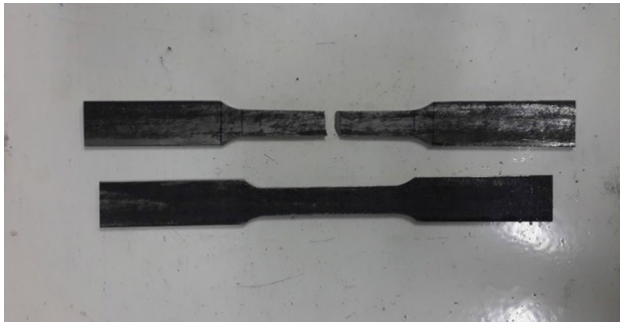


Fig. 6 The steel belt prepared for the tensile test

the sample bore the maximum force equal to 72 kN, and after that, the bearing capacity decreased. Also, in the left side loading and the 3% drift, the sample bore the maximum force equal to 86 kN, and after that, the bearing capacity decreased. After the graph drops down to 85% of the maximum force in the 4% drift, the test did not stop and continued in a cyclic form until the 10% drift. The reason for the continuation of the test was the observation of the frame behavior in very high drifts and the observation of concrete crushing.

The hysteresis diagram of force–displacement and the progression of the MRF-J sample crack in different cycles are shown in Fig. 9. By continuing this process until the 0.5% drift, no cracks were observed. That could be due to this reason that the initial cracks were covered by the steel jackets and were not observable. Based on the strain gauges results, the first plastic hinge was formed in the top bar of the beam at the connection point to the right side column. By finishing the 1% drift, the first cracks were seen in the panel zone. By continuing the loading until the 2% drift, new cracks appeared in the panel zone and the previous ones got wider and the frame recorded the maximum force

borne equal to 72.01 kN and after that the bearing capacity of the frame decreased. In this test, due to the presence of the steel jackets, the shear stress applied to the panel zone increased, and the panel zone was not able to bear the forces, and the plastic hinge occurred in the panel zone instead of the beams, and it also led to decrease the early force of the sample. After the graph drops down to 85% of the maximum force in the 5% drift, the experiment did not stop and continued until the 10% drift in the form of cyclic. The reason for the continuation of the test was the observation of the frame behavior in very high drifts and the observation of concrete crushing.

The hysteresis diagram of force–displacement and the progression of the MRF-X sample crack in different cycles are shown in Fig. 10. In this sample, the first crack occurs in the 0.25% drift in the left-hand panel zone subjected to the force of 46 kN and the displacement of 1.3 mm. Also, in the 0.5 drift the first crack of the column is created in the 0.5% drift at the base of the right side column subjected the force of 63.5 kN and the displacement of 2.06 mm. In the 1% drift, a diagonal crack was appeared



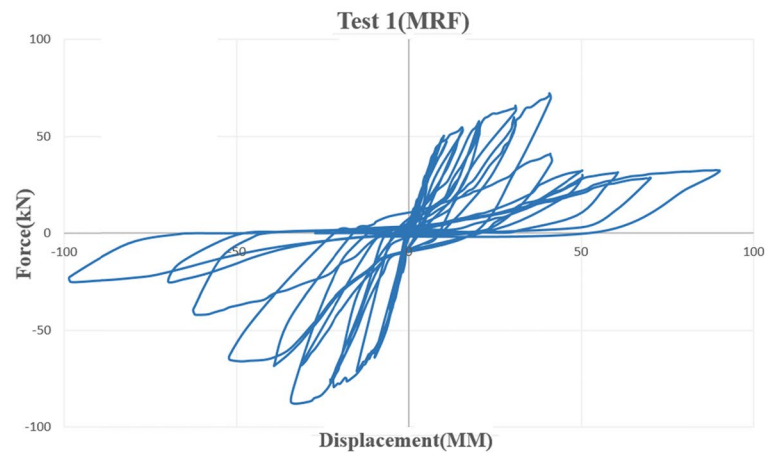
Fig. 7 Two compressive hydraulic jacks

Table 2 The results of the tensile test for steel belt

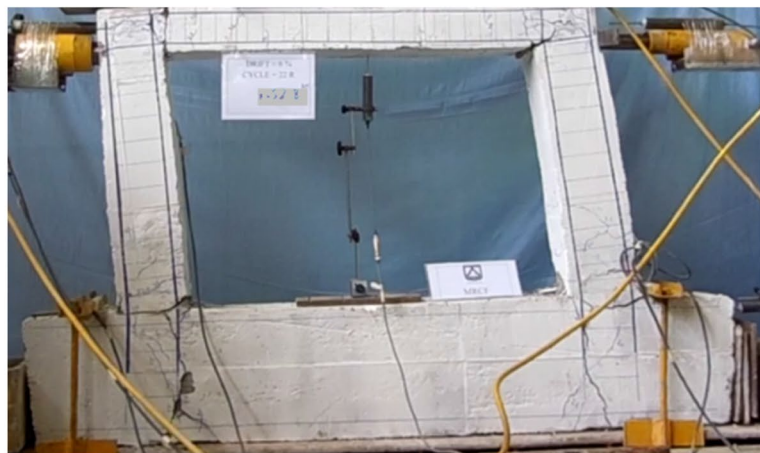
	Results		Tensile test					
	Force (N)	Extension (mm)	Stress (MPa)	Elongation (%)	Elong Aft. Brk (%)	Module (MPa)	Energy (J)	Time (Min)
Sample ID	a1							
Section type	Rectangular							
Thickness	3 (mm)							
Width	12.5 (mm)							
Gauge length	50 (mm)							
Speed	10 (mm/min)							
Peak	22,955	6.828	612.1334	13.656	13.32062	4482.523	142.5 k	1:4.73
Break	5386	9.53	143.6267	19.06	18.97931	753.5504	200.7 k	1:20.27
Yield	16,314	0.217	435.04	0.434	0.2	100,239.6	2552.755	0:0.00

Elastic module (10, 50) as long of Peak = 183,496.4 MPa

Fig. 8 The obtained results and the failure of the (MRF) specimen **a** the hysteresis diagram **b** condition of the frame at the end of loading **c** 0.25% of drift **d** 0.5% of drift **e** 4% of drift



(a)



(b)



(c)

(d)

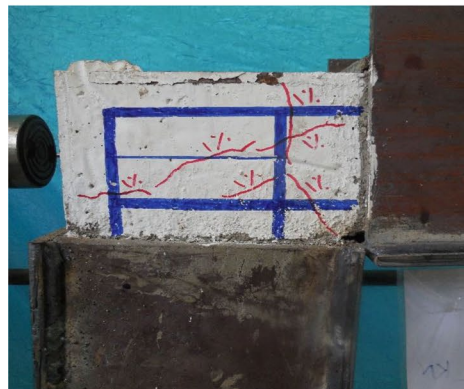
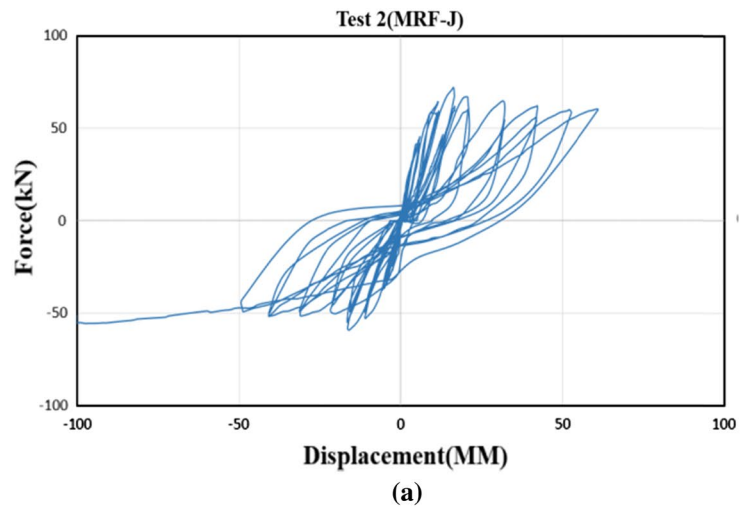
(e)

from the steel jacket edge in the left column. In the 2% drift, the number of cracks and the width of the previous cracks increase. In the 3% drift, the frame bears a force equal to 255 kN, and no sign of buckling or yield is seen in the braces. Due to the limitation of loading by one of the jacks, the loading process continues unilaterally to the left side. By continuing the loading until the 4% drift, in the displacement of 39 mm and the force of 270 kN, the compressive brace buckled out-of-plane, and subsequently the tensile brace was ruptured. By continuing the loading

until the 6% drift, the shear cracks in the column and at the edge of the steel jacket got bigger, and the crack at the steel jacket edge in the beam was also progressed. In the 8% drift, the left column is diagonally cracked, and the shear destruction occurs along the jacket.

As seen in the previous sample, due to the use of the convergent X-brace the force borne by the frame significantly increased. Now, the hysteresis diagram of force–displacement and the crack progression of the MRF-X-R sample in different cycles are shown in Fig. 11. In this

Fig. 9 The obtained results and the failure of the (MRF-J) specimen **a** the hysteresis diagram **b** condition of the frame at the end of loading **c** 1% of drift **d** 2% of drift



sample, two rings without a gap with a length of 8 cm and a thickness of 8 mm (outer diameter = 114 mm, inner diameter = 98 mm) were used at the bottom of the brace at the connection point to the corner plate. In the 0.5% drift and under the load of 89.518 kN and the displacement of 3.285 mm the first crack occurs in the left panel zone. In

the 1% drift, some cracks are created in the panel zone and the right column. Then, in the 1.5% drift and under the force of 183.203 kN and the displacement of 12.46 mm, the ring that is in the pressure is accumulated, and the tensile ring becomes an open oval (the rings are deformed). From this time, LVDT is installed on the rings to see the

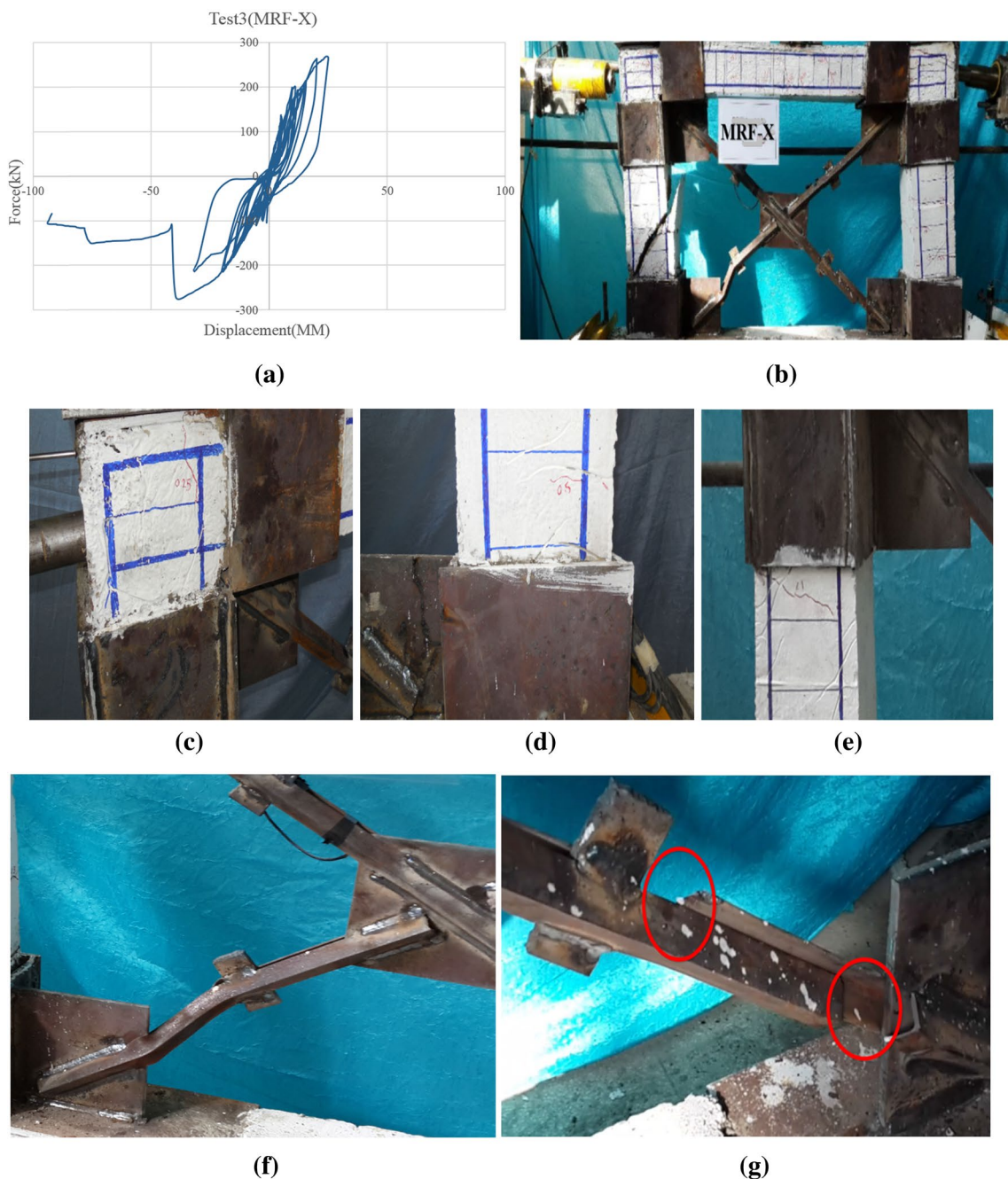


Fig. 10 The obtained results and the failure of the (MRF-X) specimen **a** the hysteresis diagram **b** condition of the frame at the end of loading **c** 0.25% of drift **d** 0.5% of drift **e** 1% of drift **f** buckling of compressive brace in 4% of drift **g** rupturing of tensile brace in 4% of drift

collapsing and opening of the rings. Subsequently, in the final cycle and the 1.5% drift and under the force of 200.04 kN and the displacement of 14.925 mm a crack was appeared along the weld line in the ring and the rings are plastic deformed. Then, in the 3% drift the ring under pressure is ruptured under the force of 104.688 kN and the displacement of 12.62 mm and the frame bearing capacity decreases. By continuing this loading, this ring is ruptured from the opposite side of the previous cut and along the

weld line and when the loading direction changes and the other ring is placed under the tension (at the same 3% drift) the ring is ruptured approximately simultaneously from both sides under a load of 108.667 kN and a displacement of 21.725 mm. The interesting note about the rings is that since the left or right loading engages two cut rings, in the loading helps the RC frame. In the 4% drift, a deep crack was appeared near the steel jacket at the base of the left column and the previous cracks get wider. In the

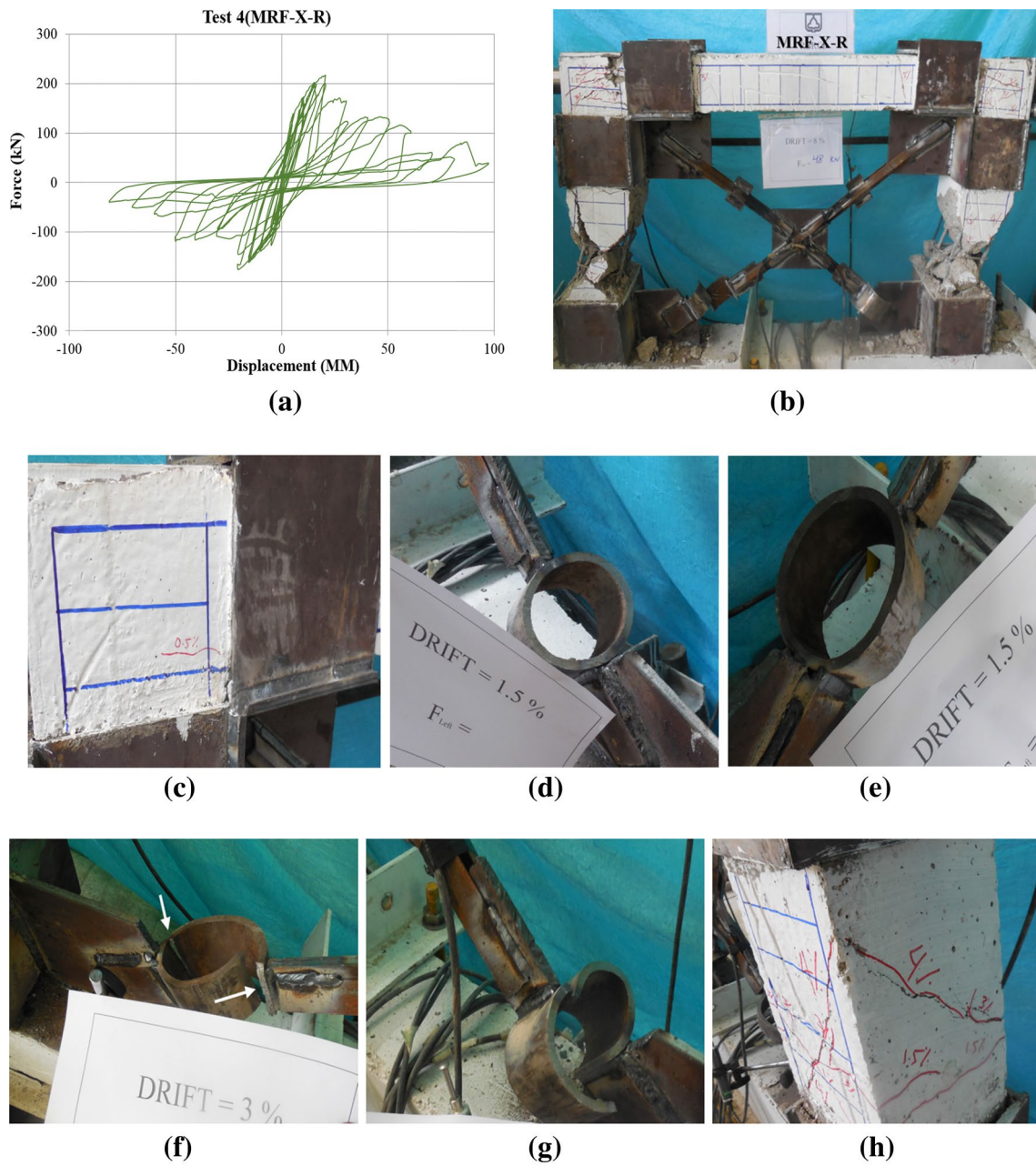


Fig. 11 The obtained results and the failure of the (MRF-X-R) specimen **a** the hysteresis diagram **b** condition of the frame at the end of loading **c** 0.5% of drift **d** the ring was compressed in 1.5% of drift **e**

elongation of the ring in 1.5% of drift **f** rupturing of the rings in 3% of drift **g** engaging two cut rings after rupturing **h** 4% of drift

followings, until the 8% drift and the complete overturning, the sample is subjected to the loading.

As shown above, in the final sample the brace remains almost intact, and the rings act as a fuse. If we want to explain the last sample, in summary, we should say that first, the rings became the bending plastic hinge. Then, the base of the left column became the shear joint, and after that, the right column base and subsequently the base of the left steel jacket were destroyed by shear.

4 Examination and evaluation of samples

In this section, based on the results obtained from the experiments, the strength, ductility, and degradation of the lateral hardness of all samples were calculated and compared with each other.

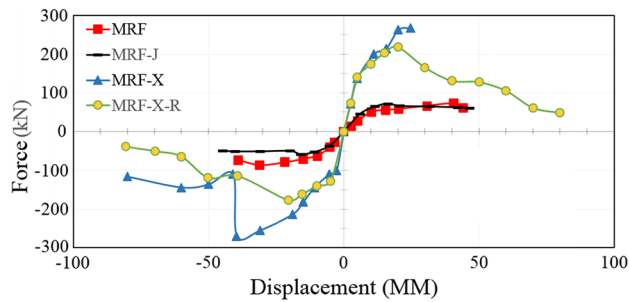


Fig. 12 The push diagram of four samples

5 Resistance

The push diagram of four samples is shown in Fig. 12. As shown, the maximum borne for the MRF-X sample was 270 kN which was 3.12 times the reference sample. Also, for the MRF-X-R and MRF-J samples, it was 2.51 and 0.83 times the reference sample, respectively.

6 Ductility

Ductility is one of the most important parameters for seismic evaluation of a structure. To obtain the ductility, using the push diagram for determining the force and the yield displacement is accompanied by some difficulties. This difficulty is due to this fact that the push diagram does not have a certain yield point. The yield point in the push diagram is not clear, and it is due to several factors including the non-linear behavior of the material and starting the yield in different parts of the structure in different levels due to the indeterminacy of the structure and re-distribution of forces [11]. For this purpose, the idealized bilinear diagram is used. Different definitions provided for drawing the idealized bilinear diagram for obtaining the yield location of structures. In this study, the method provided in Fig. 13 is used. In this method, the bilinear diagram is drawn so that the energy absorption level (the surrounded area) be the same in both diagrams.

In this method, a line parallel to the horizontal axis is drawn from the maximum force of the structure, then the line of the elastic part of the structure is drawn from the beginning of the coordinate axis to intersect the line of the maximum force. The enclosed area between two actual and ideal diagrams (energy absorption level) should be equal to each other to be representative of the actual diagram of the structure (FEMA-451 [6]). The results obtained from the bilinear diagram of the test frames are listed in Table 3.

In the above table, $\mu = \frac{u}{y}$ and $P_u = 0.85 P_{max}$. The difference between the results in two directions of go and back is due to operational problems and laboratory conditions. For

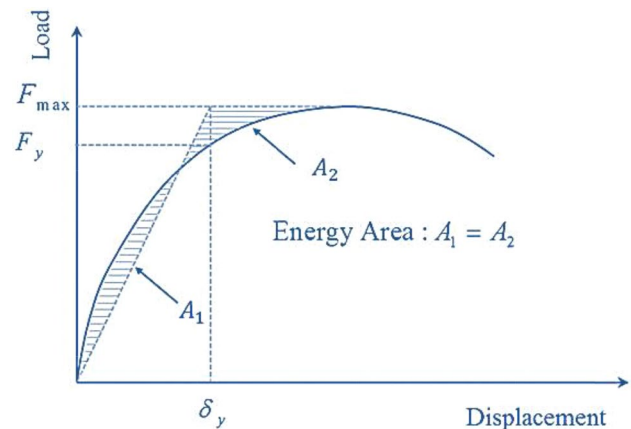


Fig. 13 The idealized bilinear diagram

the MRF-X sample, before the frame reaches to its maximum force in the right side, the loading stops on the right side, and the test continues unilaterally. Therefore, the values of the MRF-X sample in the right direction cannot be detected.

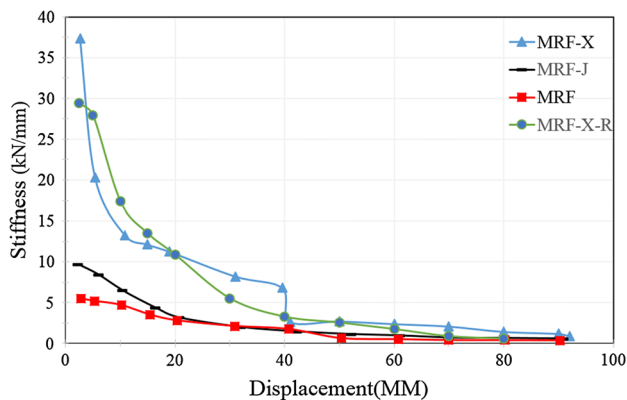
7 Deterioration of lateral stiffness

For each sample, the lateral stiffness level is calculated in each drift. The calculation trend of stiffness is by dividing the maximum force of each cycle to its corresponding displacement and is consecutively calculated for each drift. By progress during the experiment, the lateral stiffness of the frame decreases as shown in Fig. 14.

Adding the brace to the RC frame in the MRF-X sample increases the initial stiffness of the frame about 6.7 times, which is a significant value. In the MRF-X diagram, in the relative displacement of 40 mm, a severe drop is seen which is the buckling moment of the brace. At the time of removing the brace from the lateral resistance system, the stiffness of the MRF-X-R sample is a slightly more than the MRF sample and after that continues with a constant value. This excessive stiffness is due to the performance of the corner connection plates as well as the buckled brace member. In the MRF-X-R sample, the initial stiffness value is 5.35 times the reference sample stiffness which according to the more ductility than the MRF-X sample it has an acceptable stiffness. For the MRF-J sample, the frame stiffness is also 1.76 times the reference sample due to the acceptable performance of steel jackets and the stick and grout between them with concrete. Thus, using the steel jackets in this method can be assured about the complete involvement of steel jackets. The lateral stiffness of the MRF-J sample until the relative displacement of 20 mm is more than the

Table 3 Specification of yield point, peak point, ultimate point and ductility

Specimens	Loading	Yield		Peak		Ultimate		μ	$\frac{\mu}{\mu(\text{MRF})}$	$\frac{P_u}{P_u(\text{MRF})}$
		P_y (kN)	Δ_y (mm)	P_{\max} (kN)	Δ_{\max} (mm)	P_u (kN)	Δ_u (mm)			
MRF	Right	54.1	14.29	72.13	40.76	61.31	43.37	3.03	1	1
	Left	65.67	11.91	86.64	31.12	73.66	37.27	3.13	1	1
MRF-J	Right	63.68	11.29	72.24	16.4	61.4	46.65	4.13	1.36	1
	Left	52.03	10.48	59.3	15.93	50.41	44.7	4.27	1.36	0.68
MRF-X	Right	–	–	–	–	–	–	–	–	–
	Left	225.34	22.48	270	39.62	229.5	42.79	1.9	0.61	3.12
MRF-X-R	Right	170.79	9.89	217.7	20	185.04	26.4	2.67	0.88	3.02
	Left	145.67	11.75	176.67	20.49	150.17	28.9	2.46	0.79	2.04

**Fig. 14** Stiffness-displacement diagram

reference frame, and after that, they are equal to each other, and it indicates the frame stiffness increase in initial displacements by the steel jacket.

8 Conclusions

In the MRF-X sample in which the RC frame was retrofitted using the convergent steel X-brace, the frame capacity was increased about 3.12 times which brought a satisfactory result for increasing the lateral capacity. The destruction trend of this sample is so that the brace under the compressive force buckled out-of-plane and subsequently the tensile brace was ruptured. By continuing the loading after removing the steel brace from the system, shear cracks were formed in columns and caused to rupture the RC frame.

Using the steel jacket around beams and columns method for brace connection in RC structures is a suitable method, and the complete capacity of braces can be used.

Shear cracks created at the edge of steel jackets indicate a high shear force transmitted by the steel jacket to the column. To prevent early damage to columns and to increase

the frame bearing capacity, it is best to cover the columns during using them.

For using the steel jacket, the panel zone should be investigated whether the shear forces applied by the crown are bearable for it. Otherwise, using the steel jacket causes to form plastic hinges in the panel zone.

To increase the strength and the lateral stiffness of the structure, using convergent steel braces is an effective method. However, they are not efficient enough to obtain ductility. However, on the contrary, by using ductile rings without gaps in braces (sample MRF-X-R) the ductility can increase.

After completing the test related to the MRF-X-R sample, it was seen that braces remained intact and only rings were ruptured. In other words, rings were acted as fuses which are simply replaceable.

Acknowledgements The authors would like to thankfully appreciate the structural research lab of the Semnan University.

References

- Andalib Z, Kafi MA, Kheyroddin A, Bazzaz M (2014) Experimental investigation of the ductility and performance of steel rings constructed from plates. *J Constr Steel Res* 103:77–88. <https://doi.org/10.1016/j.jcsr.2014.07.016>
- ASCE (American Society of Civil Engineerings) (2005) Minimum design loads for buildings and other structures. ASCE 7-05, Reston, VA. <https://doi.org/10.1061/9780784408094>
- ATC (Applied Technology Council) (1996) Guidelines for cyclic seismic testing of components of steel structures. ATC-24. Redwood City
- Bureau of Dissemination and Promotion of National Building Regulations (2006) Iranian National Building Regulation Part-9, Design and Construction of Concrete Buildings. Publication of Iran Development, Tehran (**in Persian**)
- Dang CT, Dinh NH (2017) Experimental study on structural performance of RC exterior beam-column joints retrofitted by steel jacketing and haunch element under cyclic loading simulating earthquake excitation. *Adv Civ Eng*. <https://doi.org/10.1155/2017/9263460>

6. FEMA (Federal Emergency Management Agency) (2006) Recommended provision: design example. FEMA-451, Washington
7. Goel SC, Lee HS (1990) Seismic strengthening of structures by ductile steel bracing system. In: Proceedings of 4th U.S. National conference on earthquake engineering, 12:645–666
8. Haji M, Naderpour H, Kheyroddin A (2018) Experimental study on influence of proposed FRP-strengthening techniques on RC circular short columns considering different types of damage index. *Compos Struct* 209:112–128. <https://doi.org/10.1016/j.compstruct.2018.10.088>
9. Higashi Y, Endo T, Shimizu Y (1981) Experimental studies on retrofitting of reinforced concrete structural members. In: Proceedings of the 2nd seminar on repair and retrofit of structures, pp 126–155
10. Kheyroddin A, Khalili A, Emami E, Sharbatdar MK (2016) An innovative experimental method to upgrade performance of external weak RC joints using fused steel prop plus sheets. *Steel Compos Struct* 21(2):443–460. <https://doi.org/10.12989/scs.2016.21.2.443>
11. Maheri MR, Kousari R, Razazan M (2003) Pushover test on steel X-brace and knee-braced RC frame. *Eng Struct* 25(13):1697–1705. [https://doi.org/10.1016/S0141-0296\(03\)00150-0](https://doi.org/10.1016/S0141-0296(03)00150-0)
12. Naderpour H, Nagai K, Fakharian P, Haji M (2019) Innovative models for prediction of compressive strength of FRP-confined circular reinforced concrete columns using soft computing methods. *Compos Struct* 215:69–84. <https://doi.org/10.1016/j.composit.2019.02.048>
13. Said A, Nehdi M (2008) Rehabilitation of RC frame joints using local steel bracing. *Struct Infrastruct Eng* 4(6):431–447. <https://doi.org/10.1080/15732470600822033>
14. Sharbatdar MK, Kheyroddin A, Emami E (2012) Cyclic performance of retrofitted reinforced concrete beam-column joints using steel prop. *Constr Build Mater* 36:287–294. <https://doi.org/10.1016/j.conbuildmat.2012.04.115>
15. Sugano S, Fujimara M (1980) Seismic strengthening of existing reinforced concrete buildings. In: Proceedings of 7th world conference on earthquake engineering 4:449–456
16. TahamouliRoudsari M, Eslamimanesh MB, Entezari AR, Noori O, Torkaman M (2018) Experimental assessment of retrofitting RC moment resisting frames with ADAS and TADAS yielding dampers. *Structures* 14:75–87. <https://doi.org/10.1016/j.istruc.2018.02.005>
17. Wang W, Sheikh MN, Al-Baali AQ, Hadi MNS (2018) Compressive behaviour of partially FRP confined concrete: experimental observations and assessment of the stress-strain models. *Constr Build Mater* 192:785–797. <https://doi.org/10.1016/j.conbuildmat.2018.10.105>
18. Wyllie LA, Dal Pino JA, Cohen J (1991) Seismic upgrade preserves architecture. *Mod Steel Constr* 20-23
19. Xu CCX, Sheng PS, Wan CC (2019) Experimental and theoretical research on shear strength of seismic-damaged SRC frame columns strengthened with enveloped steel jackets. *Adv Civ Eng* 2019:1–8. <https://doi.org/10.1155/2019/6401730>
20. Yalçın C, Kaya O, Biçer E, Parvin A (2019). Retrofitting of Reinforced concrete beam-column joints by composites—part II: analytical study. *ACI Struct J* 116(1)
21. Yaseen ZM, Tran MT, Kim S, Bakhshpoori T, Deo RC (2018) Shear strength prediction of steel fiber reinforced concrete beam using hybrid intelligence models: a new approach. *Eng Struct* 177:244–255. <https://doi.org/10.1016/j.engstruct.2018.09.074>
22. Youssef MA, Ghaffarzadeh H, Nehdi M (2007) Seismic performance of RC frames with concentric internal steel bracing. *Eng Struct* 2(7):1561–1568. <https://doi.org/10.1016/j.engstruct.2006.08.027>

Publisher's Note Springer Nature remains neutral with regard to jurisdictional claims in published maps and institutional affiliations.